FRACTAL ASPECTS OF INTEGRATED CONCENTRATION FLUCTUATIONS

A. HADAD, M. STIASSNIE, M. POREH[1] and J.E. CERMAK[2]
(1) Technion- Israel Institute of Technology, Dept. of Civil Engineering, Haifa, 32000, Israel
(2) Colorado State University, Ft. Collins, Colorado, 80523, U.S.A.

(Received October 1991)

Abstract. Time series of vertically integrated concentrations (VIC) across neutrally buoyant plumes are used to study the fractal and multifractal characteristics of passive scalar fluctuations in turbulent flow fields. Here, the multifractal analysis is based on a novel definition of the singularity spectrum-$F(\alpha)$ of the time records. Approximations for quantities such as the fractal dimension and the spectral exponent are derived as functions of $F(\alpha)$ and are compared with the experimental results. Among other things, we show that VIC records are characterized by two typical subdomains. One domain, which is related to integrated concentration fluctuations, is a subfractal process; whereas the second one, which is directly related to the concentration fluctuations, is a fractal process.

1. Introduction

The phenomenon of turbulent fluctuations of passive scalars, such as concentrations, is important in various theoretical and practical problems. In air pollution problems, one is interested in the concentration fluctuations at some points in the plume, whereas in visibility obscuration problems, one is usually interested in the integrated concentrations across the plume.

The topic of concentration fluctuations is widely discussed in the scientific literature, where different approaches and models for predicting various measures which characterize the dispersion fields are suggested. These include, among others, closure models, random walk models, statistical models, and similarity models. Each of these approaches has some support by experimental measurements of concentrations, or combined measurements of concentrations and velocities.

Relatively little effort has so far been made to study integrated concentrations. Bowers and Black (1985), for example, took measurements of cross-wind integrated concentrations from plumes in the atmospheric boundary layer. The energy spectrum of these measurements was calculated by Hanna and Insley (1989) who found a 5/3 power law behavior between some bounds of wave numbers. In the present paper we refer to Poreh *et al.* (1990), who took measurements of VIC across neutrally buoyant plumes diffusing in a wind tunnel boundary layer and grid turbulence.

In the last decade investigators started to apply fractal analysis techniques in order to get new insight and understanding of turbulent fluctuations in general, and of passive scalar fluctuations in particular. So far, this analysis has been applied to various turbulent problems, such as cloud structure, flame surfaces, tracer plumes,

Boundary-Layer Meteorology **62:** 291–302, 1993.

etc. Sreenivasan (1991), gives a good survey of fractals and multifractals in fluid turbulence.

Special attention was given to the multifractal nature of the energy dissipation rate (Meneveau and Sreenivasan, 1987) and of the scalar dissipation rate (Prasad et al, 1988) in various turbulent flows, using the formalism of the singularity spectrum-$f(\alpha)$, (Halsey *et al.*, (1986)).

The present work focuses on the fractal and multifractal facets of measured time records. In section 2 we introduce a somewhat new approach for the analysis of the multifractal nature of time records. Relations between the derived singularity spectrum and other properties of the time records, such as fractal dimension and the spectral exponent are presented.

2. Theory

Turbulence is multifractal in nature, i.e., measured quantities are well described by fractal power laws (Mandelbrot, 1974; Frisch and Parisi, 1983). The bulk of existing work with multifractals is focused on the derivation of the singularity spectrum for the energy dissipation rate or the scalar dissipation rate, in various fully developed flows (Meneveau and Sreenivasan, 1987; Prasad *et al.*, 1988). Such an analysis deals with measures which are in some way related to the geometry of the measured records, but not with the geometry itself. However, the geometry of the records is multifractal. Thus, we suggest that the singularity spectrum of the measured records is the appropriate way for a multifractal analysis. Furthermore, we show that this technique is a generalization of the more common approach.

2.1. DEFINITIONS

A different formulation for the derivation of the singularity spectrum was recently proposed by Stiassnie (1991). The main steps of this formulation are summarized below. We start with a definition of a set of points which is a sampling of some continuous, bounded, single-valued function-$y(x)$, in the domain [0,1]. We divide the x-axis in the domain [0,1] into n segments of size size $\delta, n = \delta^{-1}$, and denote $x_i = i\delta$; i=0,1,....,n (Fig. 1). The number of δ-boxes which is needed to cover $y(x)$ in the domain between x_i and $x_i + \delta$ is $\triangle(x_i, \delta)/\delta$, where

$$\triangle(x_i, \delta) = y_{max}(x, \delta) - y_{min}(x, \delta), \quad x_i \leq x \leq x_i + \delta \tag{1}$$

thus, the total number of boxes-$N(\delta)$ which is needed to completely cover $y(x)$ is $\Sigma_{i=o}^{n-1} \triangle(x_i, \delta)/\delta$. The box-counting (fractal) dimension-D_b of $y(x)$ is defined and exists only when the measure M is finite:

$$M = lim_{\delta \to 0} \delta^{D_b - 1} \Sigma_{i=o}^{n-1} \triangle(x_i, \delta). \tag{2}$$

The local behavior of the function $y(x)$, in terms of the Lipschitz-Holder (L-H) exponent-α, is represented by

$$\triangle(x_i, \delta) \propto \delta^{\alpha} \tag{3}$$

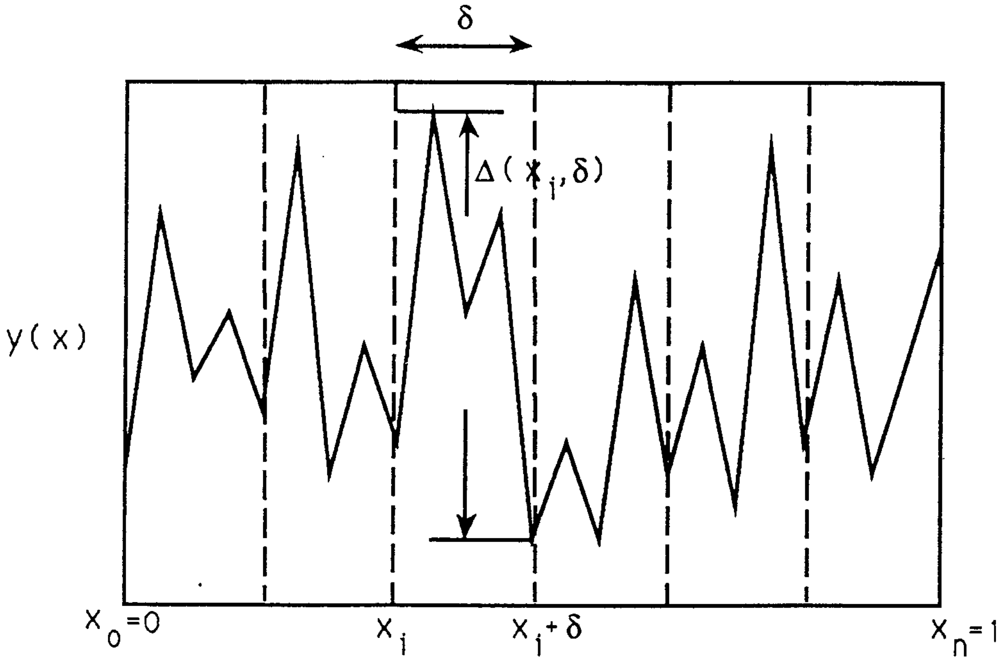

Fig. 1. Illustration of $\triangle(x_i, \delta)$.

where α determines the singularity strength, or the rate by which the derivative tends to infinity. For turbulent data we would expect $y(x)$ to have different values of α at different locations. Actually, $y(x)$ is characterized by a union of an infinite number of subsets each related to a typical singularity-α and supported by a dust on [0,1] with a fractal dimension- $F(\alpha)$. The $F(\alpha)$ curve is a 'singularity spectrum'. The number of boxes needed to cover a subset with L-H exponent between α and $\alpha + d\alpha$ is

$$N(\alpha, \delta) \propto \delta^{-F(\alpha)} d\alpha. \tag{4}$$

2.2. SINGULARITY SPECTRUM

The extension of the measure concept for multifractals is given by the q-measure of the set:

$$M_q = lim_{\delta \to 0} \delta^{\tau(q)} \Sigma_{i=o}^{n-1} \mu_i^q \tag{5}$$

where $\tau(q)$ are the 'mass exponents' and μ_i which denotes the relative weight in the i-th segment, is defined as

$$\mu_i = \triangle(x_i, \delta) / \Sigma_{i=o}^{n-1} \triangle (x_i, \delta). \tag{6}$$

From eqs. (2), (3) and (6) we get an expression for the relative weight in a segment as a function of its L-H exponent and of the box-counting dimension:

$$\mu(\alpha, \delta) \propto \delta^{\alpha + D_b - 1}. \tag{7}$$

Using eqs. (4) and (7) we can write the q-measure in the form

$$M_q \propto lim_{\delta \to 0} \int_0^\infty d\alpha \delta^{-F(\alpha)+(\alpha+D_b-1)q+\tau(q)}. \tag{8}$$

The integral in eq. (8) is calculated by the steepest descent approximation. In the limit of small δ this integral is dominated by

$$M_q \propto \delta^{-F(\alpha)+(\alpha+D_b-1)q+\tau(q)}; \quad \alpha = \alpha(q) \tag{9}$$

where $F'(\alpha) = q$ and $F"(\alpha) < 0$. The measure M_q in eq. (9) is finite only when

$$F(\alpha) = (\alpha + D_b - 1)q + \tau(q) \qquad (a) \qquad (10)$$

taking the derivative of eq. (10.a) with respect to q we find

$$\alpha = 1 - D_b - d\tau(q)/dq. \qquad (b)$$

Eqs. (10.a) and (10.b) define the singularity spectrum $F(\alpha)$, when the mass exponents curve $\tau(q)$ and the fractal dimension D_b of the set are known.

In the literature on turbulence the multifractal analysis is usually related to the dissipation rate of energy or scalars, i.e., the relative weight in a segment is given by

$$\mu_i = \frac{\int_{xi}^{x_i+\delta}(dy/dx)^2 dx}{\int_0^1 (dy/dx)^2 dx}. \tag{11}$$

In terms of the formalism of the singularity spectrum, the common notation is

$$f(\alpha) = \alpha q + \tau(q) \qquad (a) \qquad (12)$$

$$\alpha = -d\tau(q)/dq \qquad (b)$$

where α and q are the same as before, and $\tau(q)$ is slightly different due to the different definition of the relative weight in a segment. Note that if one defines a new process Y=$\int_0^x (dy/dx)^2 dx$, it can be shown that D_b of this process is unity and that eqs. (10.a,b) yield eqs. (12.a,b) which renders $f(\alpha) = F(\alpha)$.

2.3. THE FRACTAL DIMENSION

From eqs. (2),(3) and (4) one finds that

$$M \propto lim_{\delta \to 0} \delta^{D_b - 1} \int_0^\infty d\alpha \delta^{-F(\alpha)} \delta^\alpha. \tag{13}$$

Using the method of steepest descent and the fact that M has a finite value, one gets

$$D_b = 1 - \alpha_1 + F(\alpha_1); \qquad dF(\alpha)/d\alpha_{|\alpha=\alpha_1} = 1 \tag{14}$$

where α_q is used for $\alpha(q)$.

2.4. THE SPECTRAL EXPONENT

Here, we are looking for the value of the spectral exponent-β in the inertial-subrange where the spectrum is expected to follow a power law of the form $k^{-\beta}$. We estimate the spectral exponent by applying the notion of the structure function:

$$< \Delta^p(x_i, \delta) > \;\propto\; \delta^{\zeta p} \tag{15}$$

where ζp is the scaling exponent and $<>$ stands for an average over all segments. Since the number of segments in the domain is δ^{-1}, with p=2 we obtain from eqs. (3), (4) and (15)

$$< \Delta^2(x_i, \delta) > \;\propto\; lim_{\delta \to 0} \int_0^\infty d\alpha \frac{\delta^{-F(\alpha)}}{\delta^{-1}} (\delta^\alpha)^2 \tag{16}$$

which yields

$$< \Delta^2(x_i, \delta) > \;\propto\; \delta^{-F(\alpha_2)+2\alpha_2+1}; \quad dF(\alpha)/d\alpha_{|\alpha=\alpha_2} = 2. \tag{17}$$

Thus, the spectral exponent in wave number space satisfies

$$\beta = 2 + 2\alpha_2 - F(\alpha_2). \tag{18}$$

Using a parabolic approximation for F(α), eqs. (18) and (14) yield

$$\beta = 3 - 2D_b + 2F(\alpha_1). \tag{19}$$

Since the fractal dimension has values in the range $1 \leq D_b \leq 2$, and since $F(\alpha_1)_{max} = 1$, we conclude that the spectral exponent is bounded by $-1 + 2F(\alpha_1) \leq \beta \leq 3$. Exponents lower than the lower limit represent nonphysical processes, and exponents higher than the higher limit represent a non fractal process. For example, $3 \leq \beta \leq 4$ gives a process with dimension one; but the first derivative of this process is a fractal. Such a process is called subfractal.

3. Experimental work

We apply the theoretical procedure outlined in above to measured records of Vertically Integrated Concentrations (VIC) across buoyant plumes from a continuous point source. The VIC is defined as

$$VIC(x, y, t) = \int_0^\infty C(x, y, z, t) dz. \tag{20}$$

The experimental system used for measuring VIC works on the principle of absorption of IR radiation across a carbon-dioxide plume (Poreh and Cermak, 1987).

Using this experimental system we took measurements of VIC at different locations in the down and cross-wind directions. Here we concentrate on analyzing

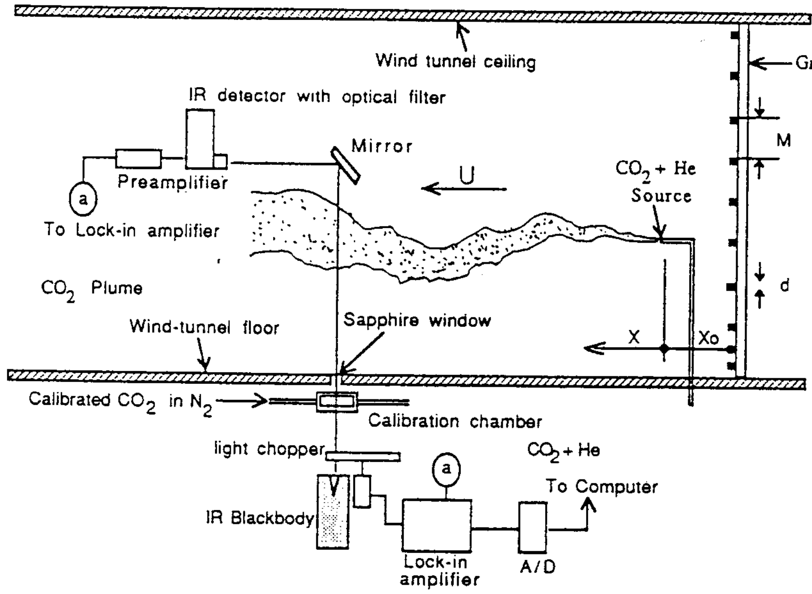

Fig. 2. Schematic description of the experimental setup for measuring VIC. Grid turbulence configuration. M=7.62cm; d=1.51cm (porosity=0.64); U=2.4m/s.

one single typical time record of VIC fluctuations across a plume diffusing in a grid-generated turbulence configuration (Fig. 2).

A time series of 256 samples which are part of this record is shown in Fig. 3. This measurement series was taken at a down-wind distance x/M=62.3 from the tracer source, and in the center-line of the plume. The complete record consists of 8000 measurements sampled at a rate of 300Hz, which yields a measurement duration of about 840M/U (U=2.4m/s) and measurement resolution, in terms of the down-wind displacement between samples, of about 8mm.

A significant length-scale of the dispersing plume is the standard deviation- σ_y of the average cross-wind plume, which for the above down-wind distance was found to be 55.2 mm. We shall use the value of σ_y as a reference length-scale in our calculations.

4. Data Analysis

The above mentioned VIC time record was processed using different statistical, spectral, and fractal tests, which are discussed below. Starting with spectral analysis, Fig. 4 shows a spectral density curve of the VIC time record in terms of non-dimensional scalar 'energy density'- S(m)=S(m)UN$\Delta t/(\sigma_{VIC}^2\sigma_y)$ vs. cycles $m^* = m\sigma_y/(UN \triangle t)$, where N denotes the number of points in the record, Δt the time step between two sampling points, σ_{VIC} the standard deviation of the VIC record at the point of measurement,σ_y the standard deviation of the cross-wind average plume, and U the average wind in the tunnel. From the spectral analysis it appears that the VIC process is characterized by two typical subdomains. In terms of

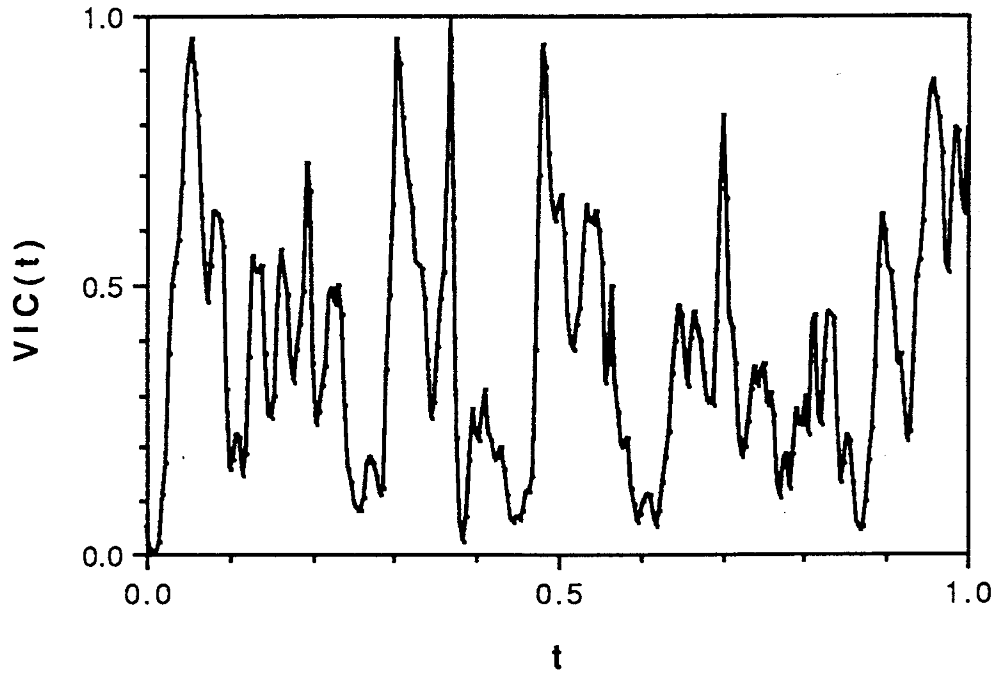

Fig. 3. A typical section of the VIC time record from grid-generated turbulence. x/M=62.3; y/σ_y=0; σ_y=55.2mm

wave lengths the transition between the domains is around σ_y. In range II (see Fig. 4) of length-scales between σ_y and about $5\sigma_y$ (i.e., of order of magnitude of the width of the average plume) we find a spectral exponent of 5/3, similar to what is usually observed in spectra of velocities and concentrations in the inertial subrange. In range I (see Fig. 4) of length-scales between $0.3\sigma_y$ (which corresponds to the Nyquist frequency of the measurement resolution and is longer than both the IR beam diameter and the smallest eddy in the field) and σ_y, we find a spectral exponent of 11/3. From this behavior we conclude that, from the point of view of the cascade, our measurements are indifferent to the integration for scales greater than the integration length, and therefore range II reflects concentration fluctuations. Hence we find a 5/3 law above length-scales around σ_y, whereas below that value, the integration yields a (5/3+2) law.

Spectral power law decay is an indication of a singular or fractal nature. If our VIC record had been a monofractal set, we would expect it to have a fractal dimension $D = (5 - \beta)/2$, (see eq. (19)), which yields values of 2/3 in the range I, and 5/3 in the range II. We would also expect it to have a singularity or Lipschitz-Holder (L-H) exponent $\alpha = 2 - D$, which yields values of 4/3 in range I, and 1/3 in range II. But, since our VIC records are embedded in two-dimensional space, its fractal dimension can vary between 1 and 2, and hence its L-H exponent varies between 0 and 1 respectively. We thus conclude that the process in range I is subfractal, whereas the process in range II is fractal. In other words, we claim that integrated concentration fluctuations are subfractal processes, whereas concentration fluctuations yield a fractal process. Therefore the discussion of the

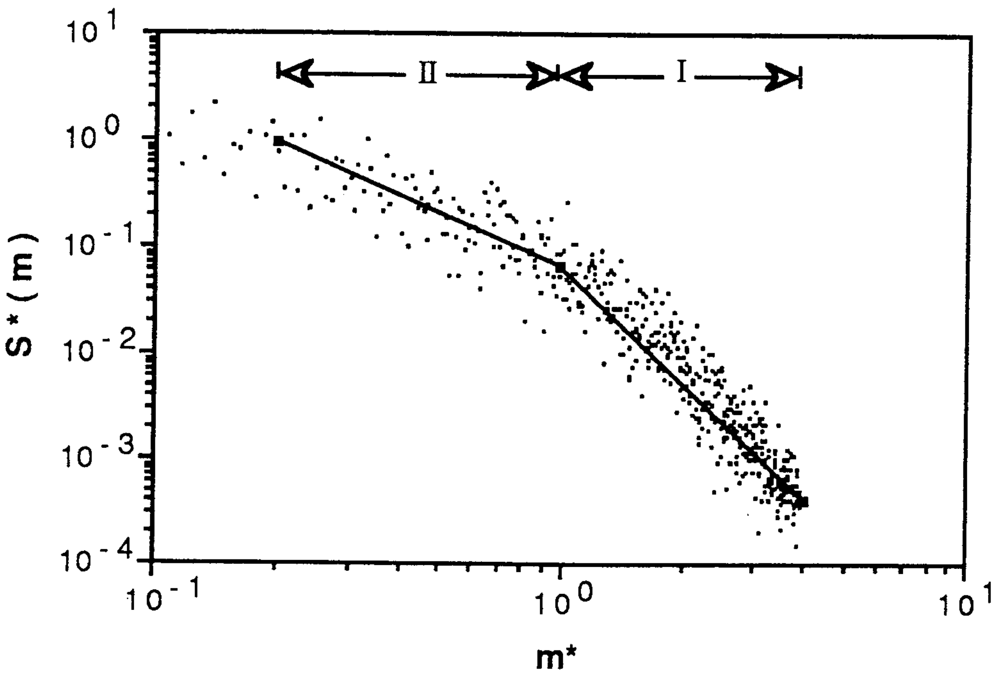

Fig. 4. Spectral density curve of the VIC time record. Non-dimensional scalar 'energy density' vs. cycles. (.) An average of 7 subsets of 1024 sampling points each. (—) Theoretical estimate. Horizontal axis in terms of wave lengths is estimated by σ_y/m^*.

fractal and multifractal nature of the VIC record will be limited to range II, which maintains its fractal nature. However, turbulent processes are multifractal in nature. This should be reflected in the singularity spectrum-$F(\alpha)$ of the record. Since the $F(\alpha)$ curve depends on the box-dimension-D_b of the record, we apply the box-counting algorithm to calculate D_b first.

According to eq. (2) D_b is equal to the slope of the curve $logN(\delta)$ vs. $\log(\delta^{-1})$ in the appropriate wavelength range. Fig. 5 shows, in terms of non-dimensional variables $N = \Sigma_{i=0}^{n-1} \triangle (x_i, \delta)/(\delta^* \sigma_{VIC})$ vs. $\delta^* = \delta U/\sigma_y$, the number of boxes of size δ needed to cover our VIC record in range II. In terms of wave lengths we find self-similarity in a range between σ_y and $15\sigma_y$. The slope of the curve, i.e., the box-dimension D_b, in this range was found to be 1.62 ± 0.03.

Using eqs. (10a) and (10b) with the above value of D_b we have calculated the singularity spectrum $F(\alpha)$. In Fig. 6 we show the singularity spectrum of the given VIC record in range II. As we could expect, α varies in the range 0 to 1, with α_{min}=0.105 and α_{max} = 0.917. The dimension F, on the other hand, is limited by the value of 1; the value of α where $F = 1$ (denoted by α_0) is the most probable value of α along the record. Here we find α_o=0.422. The value of the box-dimension is recalculated using eq. (14). From Fig. 6 we find α_1=0.343 and $F(\alpha_1)$=0.963, which yields $D_b = 1.620$. This serves as a check for the robustness of the numerical procedure. The value of the spectral exponent, independent of the spectral analysis, is calculated using eq. (18). From Fig. 6 we find α_2=0.285 and $F(\alpha_2)$=0.877, which yields $\beta = 1.693$. We find that this value is very close to 1.667 obtained from the classical Kolmogrov's 5/3 law.

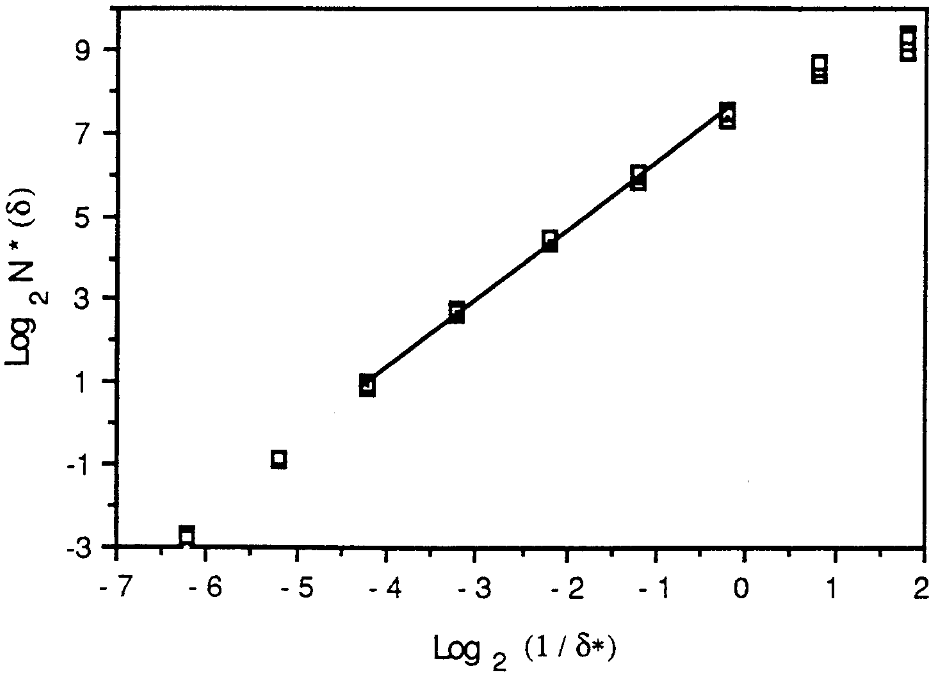

Fig. 5. Box-counting algorithm. Non-dimensional number of boxes of size δ needed to cover the given VIC record in range II: (□)7 subsets of 1024 sampling points each. (—) The average box-dimension D_b of all subsets is 1.62±0.03. Horizontal axis in terms of wave lengths is estimated by $\delta^* \sigma_y$.

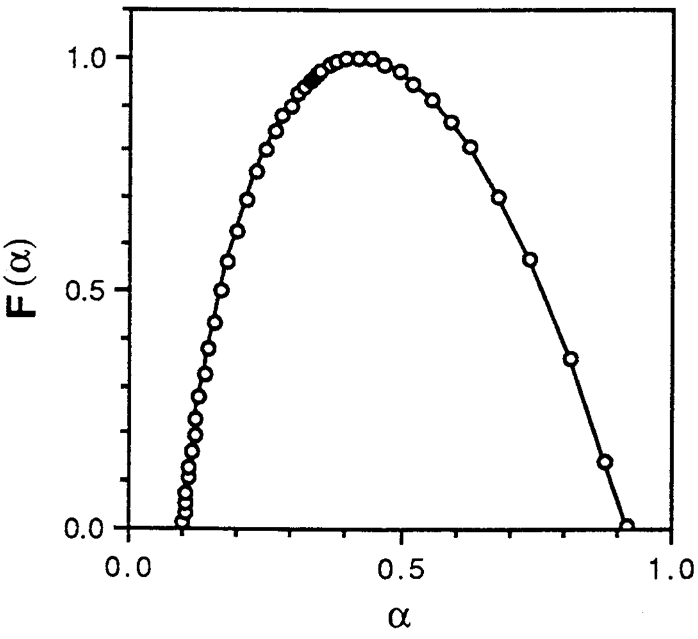

Fig. 6. The singularity spectrum $F(\alpha)$ of the given VIC record in range II.

At this stage we compare our data with other available results, which are mainly related to the dissipation rate. In Fig. 7 we present $f(\alpha)$ for our VIC record and compare it with results from velocity time series of fully developed flows, spatial

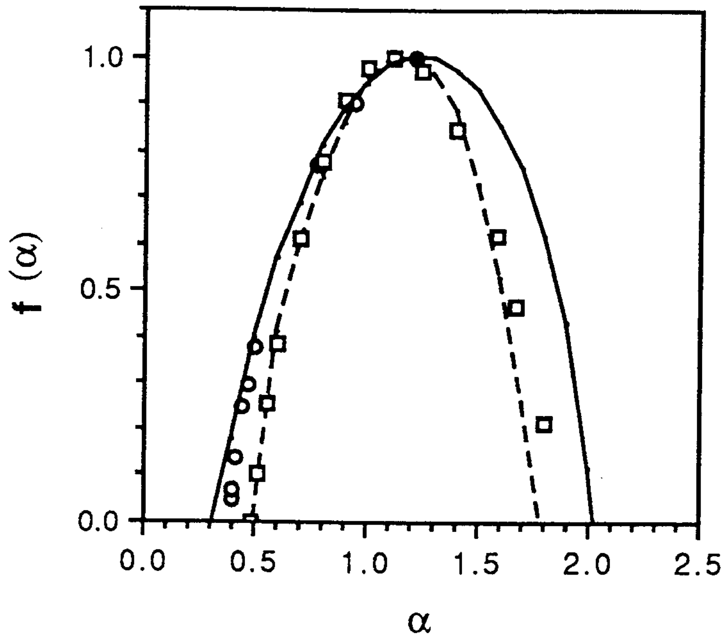

Fig. 7. Singularity spectrum f(α) of the dissipation rate from different experiments; (- - -) Velocity time series (Meneveau and Sreenivasan, 1987); (——) Spatial instantaneous pictures of concentrations (Prasad *et al.*, 1988); (o) Temperature time series (Prasad *et al.*, 1988); (□) Our VIC record in range II.

instantaneous pictures of concentrations, and temperature time series. Our results for the VIC measurements agree better with the energy dissipation rate results than with those for the so-called concentration dissipation. We have no explanation for this somewhat surprising fact. Last we compare both $F(\alpha)$ and $f(\alpha)$ from our VIC record in range II (Fig. 8). The $f(\alpha)$ curve is exactly as that in Fig. 7, i.e. its measure is based on $[\mathrm{d(VIC)/d}t]^2$. On the other hand, from considerations already mentioned in section 2.2, $F(\alpha)$ in Fig. 8 is calculated for the accumulated dissipation along the record. The excellent agreement between the two curves is rather reassuring.

5. Summary and Conclusions

Measurements of VIC fluctuations across a plume diffusing in grid-generated turbulence were analyzed. Spectral analysis provided evidence that the measurements are invariant to integration for length-scales greater than the integration length-scale, i.e. the length-scale of the plume. It appears that VIC records are characterized by two typical subdomains. The first is related to integrated concentration fluctuations and is indicative of a subfractal process, whereas the second subdomain is related to the concentration fluctuations and is indicative of a fractal process.

Multifractal analysis indicates that VIC records, in the range where the VIC reflects concentration fluctuations, are multifractal and singular everywhere. These conclusions are substantiated by the singularity spectrum-$F(\alpha)$ of the record. The $F(\alpha)$ spectrum is related to the scaling properties of the "statistical moments".

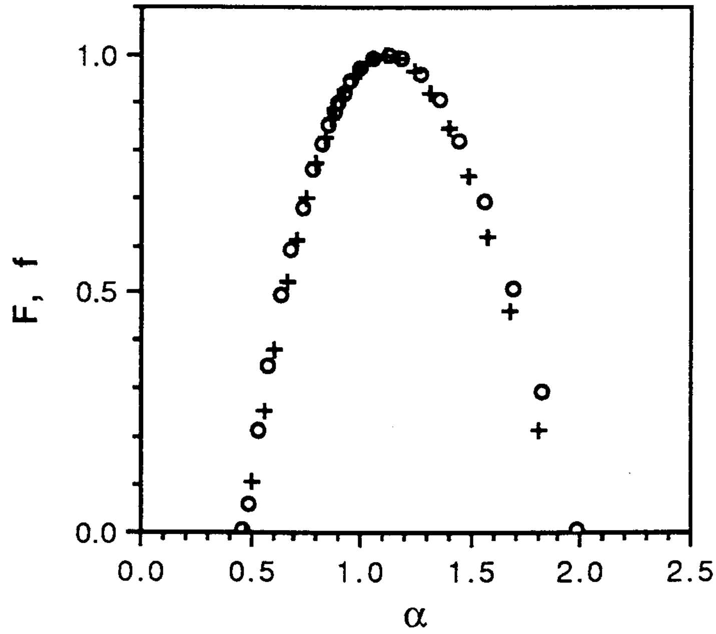

Fig. 8. Comparison between F(α)(o) vs. f(α)(+) in range II.

The first two "moments" are related to the fractal box-dimension and to the spectral exponent respectively. For the given VIC record, in the range which reflects concentration fluctuations, we found that $D_b = 1.62 \pm 0.03$ and $\beta = 1.69$. These values are in agreement with corresponding results obtained by the box-counting algorithm and spectral analysis.

Comparison between our findings and others' work shows that the $f(\alpha)$ curve for VIC is in better agreement with the $f(\alpha)$ curve for velocity fluctuations, than with that of passive scalar fluctuations.

In the future we hope to compare $F(\alpha)$ curves of velocity and VIC fluctuations. Such a comparison will give us a better understanding of the scaling nature of turbulent fluctuations in general and of passive scalar fluctuations in particular.

6. Acknowledgements

The work has been sponsored in part by the Chemical Research, Development and Engineering Center, Department of the Army, Aberdeen Proving Ground, Maryland.

The contribution of Mrs. Z. Vider in the analysis of the data and the preparation of the graphs is gratefully acknowledged.

References

Bowers J.F. and Black R.B. (1985). *Test report-product improved M3A3 (M3A3E2) smoke generator (mobile applications)*. U.S. Army Dugway Proving Ground, Dugway, UT 84022-5000.

Frisch U. and Parisi G. (1985). *On the singularity structure of fully developed turbulence*. Turbulence and predictability in Geophysical Fluid Dynamics and Climate Dynamics, New York, 84-88.

Halsey T.C., Jensen M.H. Kadanoff L.P., Procaccia I. and Shraiman B.I. (1986). *Fractal measures and their singularities: The characterization of strange sets*, Phys. Rev. **A 33**, 1141-51.

Hanna S. R. and Insley E.M. (1989). *Time series analysis of concentration and wind fluctuations*. Bound. Layer Meteor. **47** 131-147.

Mandelbrot B.B. (1974). *Intermittent turbulence in self-similar cascades: Divergence of high moments and dimensions of the carrier*. J. Fluid Mech. **62**, 331-358.

Meneveau C. and Sreenivasan K.R. (1987). *The multifractal spectrum of the dissipation field in turbulent flows*. Nucl. Phys. B. **2**, 49-76.

Poreh M. and Cermak J.E. (1987). *Experimental study of aerosol plume dynamics-III, Wind tunnel simulation of Vertical Integrated Concentration fluctuations*, CSU Project No. 5-3 2571 CER87-88MP-JEC4.

Poreh M., Hadad A. and Cermak J.E. (1990). *Fluctuations of line integrated concentrations across plume diffusing in grid generated turbulence*, CSU Project No. 5-3 8765 CER91-92MP-AH-JEC2.

Prasad R.R., Meneveau C. and Sreenivasan K.R. (1988). *Multifractal nature of the dissipation field of passive scalars in fully developed turbulent flows*. Amer. Phys. Soc. **61**, 74-77.

Sreenivasan K.R. (1991). *Fractals and multifractals in fluid turbulence*. Annu. Rev. Fluid. Mech. **23**, 539-600.

Stiassnie M. (1991). *The multifractal structure of the ocean surface*. Proceedings of the Nonlinear Water Waves Workshop. Bristol 22-25 Oct. 1991.